Journal of Optoelectronics and Advanced Materials Vol. 7, No. 2, April 2005, p. 1029 - 1038

THREE-DIMENSIONAL MEASUREMENT AND DEFECT DETECTION BASED ON SINGLE IMAGE

L. Song*, X. Qu, K. Xu, L. Lv

State Key Laboratory of Precision Measuring Technology and Instrument,
TianJin University, 300072 TianJin, China

Three-dimensional measurement and defect detection is an effective guarantee for improving the product quality. In this paper, we present a new 3-D overall measurement method using only one image, which can be effectively used in the defect detection. Compared with the former defect technology, such as the eddy current technology, the leakage of magnetic technology, the infrared technology, and the radial technology, our defect detection method is low cost, easy to operate, and can be expanded widely. The main device in the detection system is a CCD. When fixed the CCD in the workstation, CCD can capture the image of each workpiece. From the single image, we can get the three-dimensional data of the workpiece's shape ranged from 0° to 180°. Moreover, it can give an overall recognition of plane dimensions and depth information of the defect. The main working theory is, according to the 3D cues, "shading value" information left by single measurement image. According to shading, we can acquire the workpiece slant and tilt of every point's normal in the light source system of coordinates, and then transferring it to the image system of coordinates, calculating the depth information by slant and tilt. Compared with the former three-dimensional shape recovery method based on single image, this method has great improvement on the design of optical system, such as improving three-dimensional recovery accuracy and speed, with the simplification of the arithmetic, and first apply it to the industrial environment detection of defect. The three-dimensional detection method of defects, mentioned in this paper, has advantages of simple working pattern and workpiece configuration that just needs light source, CCD, image-collection card and computer, which greatly reduces the cost, and is good for use in industrial application.

(Received December 8, 2004, after revision February 7, 2005; accepted March 23, 2003)

Keywords: Defect, Detection of defects, Tonal value, Slant, Tilt

1. Introduction

The detection of defects ensures the improving of the product quality, and has a positive effect upon decreasing or avoiding the accidents brought by defects. The traditional manual detection of defects must be gradually replaced by the precise automatic detection of defects, owing to its many negative factors, such as its slow speed, the constraint of the working environments, and its disadvantage of tedious, tiring work. So far, many methods of detecting the defects have been used all over the world. The most important technologies are:

(1) The eddy current detection technique. In 1989, a factory in France designed an eddy detecting equipment called EDISOL installed at the front part of fire-cutting equipment,

* Corresponding author: lilymay1976@126.com

which could examine simultaneously the surface of the board without damage. However, its demand of big magnetizing current caused the waste of resource and the pollution of the electrical wire. In 2003, ShanDong Province Victory Powerhouse in China detected the defect of a coagulator with the eddy detecting technique; only got the results of the interior and exterior surface nick missing the trivial impenetrating defects.

(2) The leaky magnetic detecting technique. In 1993, ChuanQi from iron product factory in Japan exploited the simultaneous examining non-metal mixture equipment. In 2003, the Mechanism Collage and Tianjin University in China both have implemented the detection of the pipeline inner defects by examining the leaky magnetic flux induced by the defect of the magnetized metal channel to get the information about the damage degree of the channel. The leaky magnetic detecting technique manifests its advantage at the detecting great pipeline defect, while exposes its weakness at the detecting the 3D defect of common workpiece and the pipeline, which can't be magnetized.

(3) The infrared technique. Norwegian Elkem Company designed Therm-O-Matic automatic detecting system in 1990. This technique is applicable for the field where the temperature varied obviously at the defects. In 2003, Tianjin Petrochemical Company in China examined the heat pipeline defect with this method, and analysed the corrodent plot whose diameter is longer than 2m, while could not deal with the wide corrodent area or the trivial cracks.

(4) X-ray and ultrasonic methods are applied to the detecting the workpiece without damage to some degree. However, this technique lacks high resolution; it cannot applied for the surface defect detection.

(5) Visual detection. Computer Visual Detection has become the prevailing study subject all over the world recent years. In 1995, Japanese succeeded in applying the Computer Visual System based on laser scan to QianYe factory and ChuanQi factory. In 2003, a university in China established the defect detection system of steel surface by the local analysis and computer visual extraction approach. With the control of the angle between the light source direction and the camcorder, the image can be collected both in the bright area where the mark of oil, water and spot can be detected and in the dark area where the trivial cracks and abrasions can be detected. However, the method is limited in the field of plane detection and the depth information on the defects is lacking. Using image approaches, the surface defect can be detected; unfortunately, the defects depth cannot be revealed.

The defect detection technique mentioned in this paper isn't a detection that just picks up local points or local surface to examine, but detection the overall 3D shape information. The 3D detection has become a new aim in the field of measurement. Though a great many studies on the recovery of 3D shape have been processed now, most of them just stopped at the lab stage, and couldn't practice into the automatic production working line because of constraints of precision, measuring range, working condition, and producing process. No practical production for 3D defect detection was developed till now.

This paper indicates that SFS (Shape from shading) technique [1] is simple and available to be used in the industry, after researching on a great many methods of 3D shape recovery. However, so far, this method is just in its beginning moment and its precision is very low [13]. This paper, based on the SFS method, focuses on improving the light source system and the performance of the 3D algorithms, with the result that its precision has been increased effectively. With the application of SFS to the 3D defect detection of certain magnetic material, the process of detection has been simplified as follows: avoiding the complicated measurement of distance in traditional methods, this method is based on a workpiece's photograph measured simultaneously to recover the 3D shape. The tools required are very few, which just needs a visual sensor, image picking cards, the light source, and computer. In few words, this method increases the speed and lowers the cost, available to the practical industrial production.

2. The analysis of the 3D shape recovery based on single image

The image in computer contains various informations, such as shading [2], outline, texture [12] and so on. Shading [3] plays an important role in human perception of surface shape. The first SFS technique was developed by Horn in the early 1970s, which is famous for its original 3D shape recovery based on single image. Unfortunately, he couldn't achieve a satisfactory precision. Later, many scholars continued to improve this method and considered it as a prospective one. Thus, the precision has increased gradually. This paper studies the factors deciding the gray shading, finds the relationship between the image shading and surface normal, and then gets the surface 3D coordinates. Compared with the former SFS methods, the operation is performed more concisely; moreover, the precision of 3D shape recovery has been greatly improved.

The shading of image is influenced by four factors [4], which are illustrated in Fig. 1.

(1) The geometrical shape of the visible surface.
(2) The intensity and direction of light incident.
(3) The relative orientation and distance from observer to object.
(4) The reflection properties of the surface.

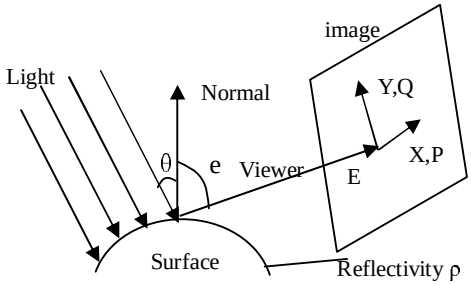

Fig. 1. Four factors influence shading value.

One assumes that the viewing direction and the normal to the x-y plane makes an angle "e" [5], and the surface gradient (P, Q) is consistent with the surface (X, Y, Z). The energy of the incident light is I (x, y), the vector of the light source direction is (p_i, q_i, -1), the vector of the surface normal is (p, q, -1), the angle between the vector of the light source direction and the vector of the surface normal is θ. So, the reflectance energy of the normal can be expressed as follows:

$$E(x,y)=I(x,y)\rho\cos\theta \tag{1}$$

In the inner space, the angle α between two random vectors x and y can be expressed as follows:

$$\cos\alpha=\frac{x\bullet y}{|x||y|} \tag{2}$$

So the cosine function of the angle between the incident light direction and the surface normal can be expressed by the formula:

$$\cos\theta=\frac{(pp_i+qq_i+1)}{\sqrt{p^2+q^2+1}\sqrt{p_i^2+q_i^2+1}} \tag{3}$$

The gray of image can be expressed as follows:

$$E(x,y)=I(x,y)\rho\frac{(pp_i+qq_i+1)}{\sqrt{p^2+q^2+1}\sqrt{p_i^2+q_i^2+1}} \tag{4}$$

We can conclude from formula (4) that the normal vector of the brightest pixel in the image points to the light source direction.

We assume that the 3D curved surface is expressed with the obvious function: z=f(x, y), and f(x, y), whose partial derivative f_x, f_y are both continuous, is the limited function in the limited closed area, the 3D shape recovery can be expressed in the following four approaches [6,7], which are illustrated in Fig. 2.

(1) Z (depth), extract every element's depth from x and y.
(2) Surface normal （n_x, n_y, n_z）. The surface normal of the curved surface: z=f(x, y) can be rewritten as （f_x, f_y, -1）.
(3) Surface gradient (p, q).
(4) Slant Φ and tilt θ.

One sets a reference frame with setting the light source direction as the z direction. From the formula (3), we can conclude that the angle Φ_i between the surface normal and light source direction of the image point can be acquired as follow:

$$\phi_i = \arccos\frac{E_i}{E_{\max}} \tag{5}$$

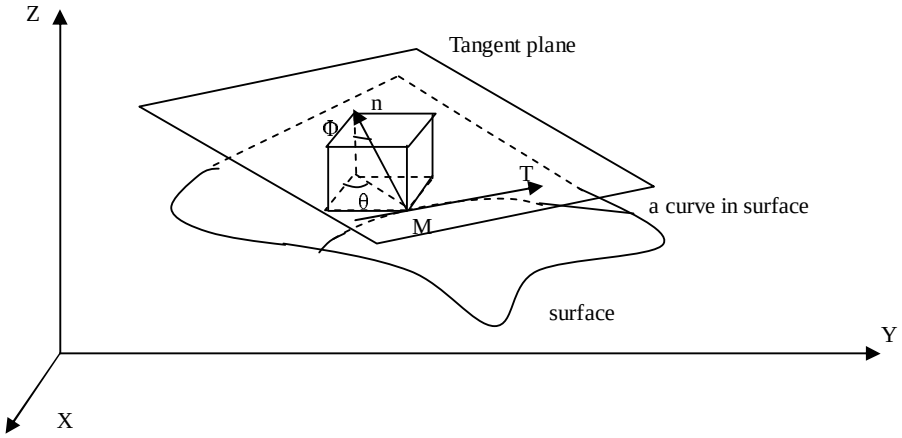

Fig. 2. Surface tangent and normal.

If the incident light energy does not vary [8], and the surface reflectance is constant, in a measuring step, the value of I and ρ can be considered as constant, without considering the time dependence. Therefore, the reflectance formula can be expressed with the coefficients of the slant and tilt such as p_s,q_s,p_i,q_i:

$$E_i = \frac{(tg\phi_s \cos\theta_s tg\phi_i \cos\theta_i + tg\phi_s \sin\theta_s tg\phi_i \sin\theta_i + 1)}{\sqrt{tg\phi_s^2 \cos\theta_s^2 + tg\phi_s^2 \sin\theta_s^2 + 1}\sqrt{tg\phi_i^2 \cos\theta_i^2 + tg\phi_i^2 \sin\theta_i^2 + 1}} \tag{6}$$

The surface of the object is assumed to be continuous, so we can assume spherical any part of the object. As a result, we can get the formula (7):

$$d\phi = \frac{\sin\phi\cos\theta dx + \sin\phi\sin\theta dy}{r\sin\phi\cos\phi} \tag{7}$$

From formula (6) and formula (7) , we get (8).

$$\theta = \arctan \frac{I_y \cos\theta_s - I_x \sin\theta_s}{I_x \cos\theta_s \cos\phi_s + I_y \cos\phi_s \sin\theta_s} \tag{8}$$

The slant and tilt can be derived separately from the formula (5) and formula (8), thereby we can obtain the 3D dimension of the surface.

3. The design of the 3D shape recovery system based on single image

The method mentioned in this paper is simple and inexpensive [9,10]. The method needs an optical system, an image collected system and a computer. The sketch map can be seen in Fig. 3.

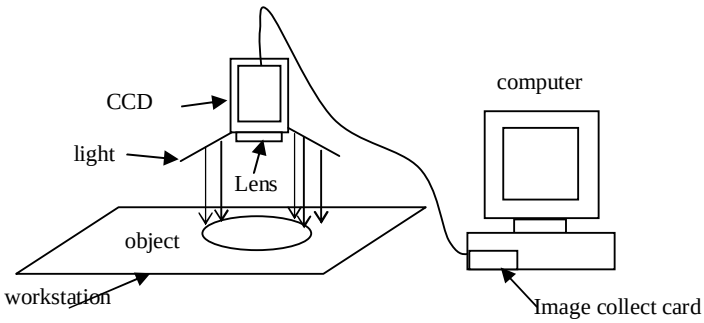

Fig. 3. Sketch map of hardware system.

The parallel light [11] is the ideal choice in this system. However, the parallel light, which can be purchased at present, has the disadvantages of too small measuring diameter of parallel light and high cost. We self-designed a “round table LED illumination system” to satisfy the demand of this method. The light beam of this optical system is explained in Fig. 4. The shape of the light source designed as round table simulates the sphericity [14], with the object setting at the focus of light source, for the sake of getting the symmetrical illumination. Five circles of photodiodes were co-located closely on the circuit board formed as round table. If the photodiodes’ radiation angle is close to zero, the lights can concentrate on the working area. The lights are distributed symmetrically on the working area plane. Thus, setting the workpiece on this plane one gets effective illumination. The distance from the light source to this plane is:

$$H = (R + r) \times ctg\beta \tag{9}$$

According to the geometrical relationship, and because $\beta = \alpha$, one obtaines:

$$H = (R + r) \times ctg\alpha \tag{10}$$

where r is the radius of the up round table formed by circuit boards, R is radius of the working area where the lights concentrate, H is the relative distance from the light source to the workpiece. If we constrain the distance H, and make sure that r keeps bigger than the radius of CCD lens, we have enough information to design the tilt and radius of circuit board.

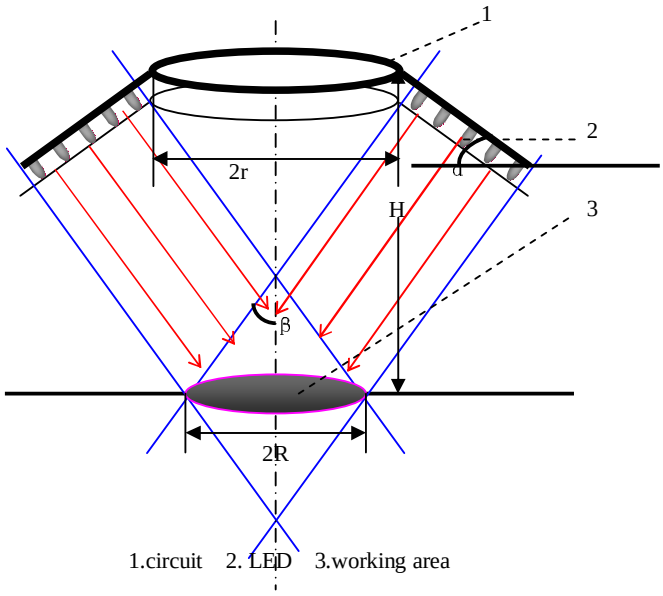

Fig. 4. Optic theory of the light system.

This light source system designed in our laboratory has good stability, symmetrical brightness, and has the ability to change the brightness by varying the voltage supply. It can fulfill the demand of the condition with a low cost design, which result is close to the Lambertian model.

In the selection of the photoelectric sensor and the image collecting system in this design, we choose MTV-1881EX camcorder produced by TaiWan MinTong Company as the image collecting system, or choose numeral camcorder, either. The distance between the collecting equipment and workpiece has no strict limitation, when the image available to measure is very good.

4. The application of 3D detection of defects

The detection of shape under way can improve the product quality effectively. Confined by the measurement and working condition, so far, little was applied to the practical industry. Just for the advantages of simple equipment and easy installment, this 3D shape recovery and defect detection system is proper to be used in the practical industry. For example, in the manufacture of magnetic materials, it is necessary to detect and reject the material's defect in time. Fig. 5 indicates the automatic 3D detection of defect product line established in industrial production. To avoid the mixed light (such as the electric arc light) influencing to the measurement result, it can be solved as follows: set a darkroom surrounded by black cloth in a proper position where detects the 3D defect of workpiece. When the measurement result remains noisy, we can adopt the image processing technique, such as smoothing technique, median filter technique, etc. The treatment of the image, can remove the noisy.

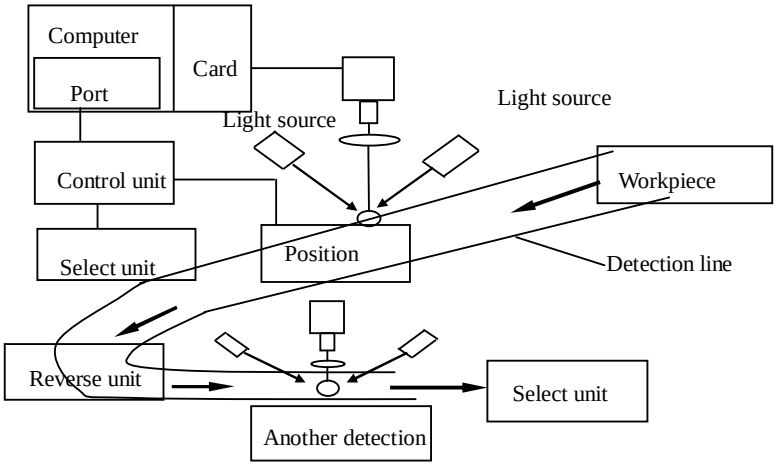

Fig. 5. 3D defect detection system.

Before measuring, the camcorder, the light source and the software parameter should be adjusted. The workpiece is sent to the assembly line and when it reaches the field for CCD collecting image, the system notices the main program by the detection of position where the workpiece is situated. The program begins to collect the image and recover the 3D shape of image. In this procedure, the main program judges that, whether the depth of every pixel has great deviation from the ideal depth, whether it the defect exists, and whether it is needed to notice the selection system to select, or not, then detecting the workpiece is put in reverse mode. The reversal detection is similar to the former. If defect exists, send it to select again, if not, send it to the none-defect box.

The photo picked up in the industrial production line, which can be seen in Fig. 6, can give us a remarkable information. We can perceive the defect's position and shape from the photo with naked eyes. At present, the plane dimension of the defect can be generally acquired by the plane image technique, except the depth dimension.

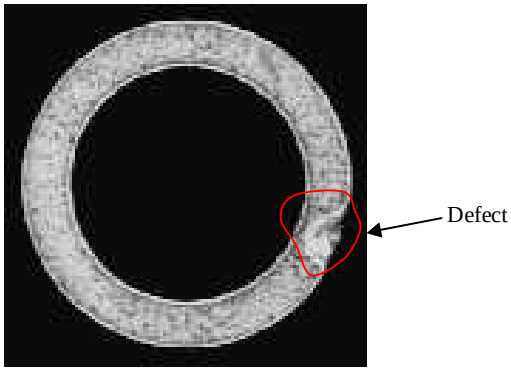

Fig. 6. Single magnetic material image.

The recovering of the 3D shape of the workpiece by the method mentioned in this paper, the 3D shape recovery technique, is based on single image. The dimensions of workpiece's plane and depth are both available. Because there are 128×128 pixels in Fig. 5, and its shape dimension is 20×20×2 mm, the recovery of 3D image subdivides the dimensions in x direction and y direction to 128 equal parts separately. The resolutions of x and y are both:

$$20/128=0.1 \text{ mm}$$

the resolution of x-y plane is:

$$（20\times20）/（128\times128）=0.02 \text{ mm}^2$$

The resolution of z direction depends on the gray level of image. As this design adopts the gray level of 256, the resolution of z direction is:

$$2/256 = 0.007 \text{ mm}$$

Fig. 7 contains 128×128 pixels. The recovery 3D image distinguishes the defect's position and shape clearly, and gives the defect's depth precisely. The 3D dimensions of 80 pixels from the defect are displayed in Table 1, with 10 lines and 8 rows. X coordinate ranges from 15.625 mm ～ 16.719 mm, Y coordinate ranges from 6.250 mm ～ 7.656 mm. The value of Z coordinate is deduced from the 3D shape recovery technique. Table 1 shows every pixel's depth information, different widely from the ideal depth: 2 mm, which has a trend of gradual decline by lines. The smallest depth in table is 0.186 mm, having a great difference from the ideal depth of 2 mm, judged as the obvious defect. According to similar means, the depth information of defect can be identified by judging the difference between the detected depth and the ideal depth.

Table 1. Some 3D dimension data of the defect in a workpiece.

ID	Measurement value (unit: X: mm, Y: mm, Z: 0.1 mm)								
1	X	15.625	15.781	15.938	16.094	16.250	16.406	16.563	16.719
	Y	6.250	6.250	6.250	6.250	6.250	6.250	6.250	6.250
	Z	16.822	15.701	16.262	15.140	12.056	14.953	11.121	1.869
2	X	15.625	15.781	15.938	16.094	16.250	16.406	16.563	16.719
	Y	6.406	6.406	6.406	6.406	6.406	6.406	6.406	6.406
	Z	14.019	14.393	17.664	17.009	13.925	12.710	12.075	3.178
3	X	15.625	15.781	15.938	16.094	16.250	16.406	16.563	16.719
	Y	6.563	6.563	6.563	6.563	6.563	6.563	6.563	6.563
	Z	18.692	17.757	15.047	13.738	12.710	14.299	11.869	2.091
4	X	15.625	15.781	15.938	16.094	16.250	16.406	16.563	16.719
	Y	6.719	6.719	6.719	6.719	6.719	6.719	6.719	6.719
	Z	18.692	15.047	13.084	13.832	17.850	17.850	14.323	7.654
5	X	15.625	15.781	15.938	16.094	16.250	16.406	16.563	16.719
	Y	6.875	6.875	6.875	6.875	6.875	6.875	6.875	6.875
	Z	8.972	17.664	14.860	10.935	10.935	9.439	12.336	9.333
6	X	15.625	15.781	15.938	16.094	16.250	16.406	16.563	16.719
	Y	7.031	7.031	7.031	7.031	7.031	7.031	7.031	7.031
	Z	9.8131	17.757	10.561	9.4393	11.682	12.991	15.514	15.981
7	X	15.625	15.781	15.938	16.094	16.250	16.406	16.563	16.719
	Y	7.188	7.188	7.188	7.188	7.188	7.188	7.188	7.188
	Z	19.252	18.411	14.299	18.692	17.009	19.346	17.383	4.579
8	X	15.625	15.781	15.938	16.094	16.250	16.406	16.563	16.719
	Y	7.344	7.344	7.344	7.344	7.344	7.344	7.344	7.344
	Z	19.439	19.626	19.252	19.159	17.757	19.720	17.477	3.925
9	X	15.625	15.781	15.938	16.094	16.250	16.406	16.563	16.719
	Y	7.500	7.500	7.500	7.500	7.500	7.500	7.500	7.500
	Z	19.533	19.533	19.720	18.318	11.776	12.991	12.523	4.589
10	X	15.625	15.781	15.938	16.094	16.250	16.406	16.563	16.719
	Y	7.656	7.656	7.656	7.656	7.656	7.656	7.656	7.656
	Z	18.505	19.346	15.140	17.290	19.533	7.757	8.911	6.065

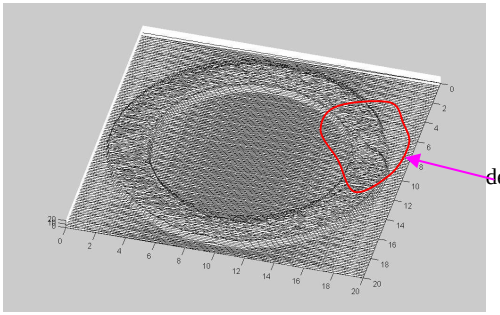

Fig. 7. 3D recovery of workpiece.

5. Conclusions

This paper deals with the 3D detection of defect on the surface of workpiece by the 3D shape recovery technique. Compared with the traditional techniques of defect detection, this one offers more complete information about defect. This method just needs measuring the single image under way, with the result that a 3D shape recovery ranged from 0 to 180 degree is obtained. It is more simple and effective than the former techniques [15], and greatly advances the speed and precision. The equipments require: light source, CCD, the image-acquiring card, and computer, which greatly lower the cost of the system, available to the industrial production.

This method has succeeded in the detection of the magnetic materials' defect. As for the workpiece's shape dimension is 20 mm×20 mm×2 mm, the resolution of X and Y has reached 0.1 mm, the resolution of Z has reached 0.007 mm, which is enough to fit for the demand of the detection of the defect in the magnetic material.

The 3D shape recovery technique used in this paper on defect detection can be also applied, widely, in other fields such as the orientation of target military area, the analysis of air bladder in chemistry, the 3D identification of people according to the photo in police, the recovery of antique objects according to photo, model manufacture field, stereo identification of words, and so on. Other 3D methods, would be of help for the analysis of the 3D information of local area.

One can observe from the above discussion that the 3D shape recovery based on single image is surely an effective and largely applicable method [16]. With the improvement of the light source and photograph condition, it is possible to raise the precision of this recovery method.

Acknowledgments

The financial support of YeShenghua, a famous academician in China, and my teacher QuXinghua, is kindly acknowledged.

References

[1] Ruo Zhang, Ping-sing Tsai, James Edwin Cryer, etc, Shape from shading: A survey, IEEE transactions on pattern analysis and machine intelligence **21**(8), 690 (1999).
[2] S. Naganuma, N. Tagawa, A. Minagawa, Estimation of 3D shape and reflectance using multiple Moire images and shading model, Proceedings of the ACM Symposium on Applied Computing, 943 (2003).
[3] J. Y. Chang, K. M. Lee, S. U. Lee, Shape from shading using graph cuts, IEEE International Conference on Image Processing **1**, 421-424 (2003).
[4] P. F. Frank, D. L. Martin, Where and shy local shading analysis works, IEEE

transactions on pattern analysis and machine intelligence **11**(2). 198 February (1989).
[5] R. Kimmel, A. M. Bruckstein, Global shape from shading, Computer vision and image understanding **62**(3), November, 360 (1995).
[6] H. Ragheb, E. R. Hancock, Darboux smoothing for shape-from-shading, Pattern Recognition Letters **24**(1-3), January, 579 (2003).
[7] S. Lu, D. Metaxas, D. Samaras, J. Oliensis, Using multiple cues for hand tracking and model refinement, Proceedings of the IEEE Computer Society Conference on Computer Vision and Pattern Recognition **2**, II/443-II/450 (2003).
[8] J. Wei, Robust recovery of multiple light source based on local light source constant constraint, Pattern Recognition Letters **24**(1-3), January, 159 (2003).
[9] Y. Wang, D. Samaras, Estimation of multiple directional light sources for synthesis of augmented reality images, Graphical Models **65**(4), July, 185 (2003).
[10] A. Robles-Kelly, A. G. Bors, E. R. Hancock, Surface acquisition from single gray-scale images, IEEE International Conference on Image Processing **3**, 721 (2003).
[11] Y. Jiang, R. N. Carrow, R. R. Duncan, Effects of Morning and Afternoon Shade in Combination with Traffic Stress on Seashore Paspalum, HortScience **38**(6), October 1218 (2003).
[12] D. I. Morales, M. Moctezuma, F. Parmiggiani, Urban and Non Urban Area Classification by Texture Characteristics and Data Fusion, International Geoscience and Remote Sensing Symposium (IGARSS) **6**, 3504-3506 (2003).
[13] E. Prados, O. Faugeras, Perspective shape from shading and viscosity solutions, Proceedings of the IEEE International Conference on Computer Vision **2**, 826 (2003).
[14] A. Tankus, N. Sochen, Y. Yeshurun, A new perspective on shape-from-shading, Proceedings of the IEEE International Conference on Computer Vision **2**, 862 (2003).
[15] T. Sawada, H. Kaneko, Spatial properties of multiple cues for perceiving shape from shading, Kyokai Joho Imeji Zasshi/Journal of the Institute of Image Information and Television Engineers **57**(5), May 597 (2003).
[16] K. Y. Bae, B. Benhabib, A hybrid scheme incorporating stereo-matching and shape-from-shading for spatial object recognition, Proceedings of the Institution of Mechanical Engineers, Part B: Journal of Engineering Manufacture **217**(11), 1533 (2003).